⌘ *Author's Choice*

A Mediator of Rho-dependent Invasion Moonlights as a Methionine Salvage Enzyme*[S]

Yukihito Kabuyama,[a,b] Elizabeth S. Litman,[a,c] Paul D. Templeton,[a] Sandra I. Metzner,[a] Eric S. Witze,[a] Gretchen M. Argast,[a,d] Stephen J. Langer,[e] Kirsi Polvinen,[a,f] Yiqun Shellman,[g] Daniel Chan,[h] John B. Shabb,[i] James E. Fitzpatrick,[g] Katheryn A. Resing,[a,†] Marcelo C. Sousa,[a] and Natalie G. Ahn[a,c,j]

RhoA controls changes in cell morphology and invasion associated with cancer phenotypes. Cell lines derived from melanoma tumors at varying stages revealed that RhoA is selectively activated in cells of metastatic origin. We describe a functional proteomics strategy to identify proteins regulated by RhoA and report a previously uncharacterized human protein, named "mediator of RhoA-dependent invasion (MRDI)," that is induced in metastatic cells by constitutive RhoA activation and promotes cell invasion. In human melanomas, MRDI localization correlated with stage, showing nuclear localization in nevi and early stage tumors and cytoplasmic localization with plasma membrane accentuation in late stage tumors. Consistent with its role in promoting cell invasion, MRDI localized to cell protrusions and leading edge membranes in cultured cells and was required for cell motility, tyrosine phosphorylation of focal adhesion kinase, and modulation of actin stress fibers. Unexpectedly MRDI had enzymatic function as an isomerase that converts the *S*-adenosylmethionine catabolite 5-methylribose 1-phosphate into 5-methylribulose 1-phosphate. The enzymatic function of MRDI was required for methionine salvage from *S*-adenosylmethionine but distinct from its function in cell invasion. Thus, mechanisms used by signal transduction pathways to control cell movement have evolved from proteins with ancient function in amino acid metabolism. ***Molecular & Cellular Proteomics 8:2308–2320, 2009.***

Cutaneous malignant melanoma has doubled in incidence over the past 30 years. Stages involved in progression of melanocytes to melanoma based on clinical and histopathological features include nontumorigenic nevi, dysplastic or atypical nevi, primary radial growth phase and vertical growth phase melanoma, and metastatic melanoma (1). Metastatic melanomas are often resistant to treatment; therefore therapeutic strategies require a more complete understanding of molecular determinants of this disease, particularly those involved in the invasive phenotype (2).

Rho GTPases control a wide range of cellular responses including cell movement, morphogenesis, and coordinated migration (3). These pathways are implicated in malignant cell transformation and metastasis based on *in vitro* evidence showing tumorigenic and invasive responses to enhanced signaling in cell lines. Studies have demonstrated that overexpression of RhoC enhances invasion and metastasis in mouse xenografts of human melanoma and lung cancer cell lines (4, 5). In addition, some human tumors show elevated expression of Rho GTPases and exchange factors and/or reduced expression of GTPase-activating factors (6–8). Signaling through RhoA promotes actin polymerization and stress fiber formation, providing cells with contractile force needed for cell movement. Rho-GTP interacts with various effectors, including Rho-activated kinase, which promotes actin-myosin assembly via phosphorylation of myosin light chain phosphatase (9), or diaphanous-related formins, which nucleate actin filaments and stabilize microtubules (10, 11). Studies of cultured melanoma cells have revealed an "amoeboid" invasion mechanism involving RhoA-dependent Rho-activated kinase activation and inactivation of Rac (12, 13).

RhoA also controls the formation and turnover of focal adhesion contacts, which mediate interactions between extracellular matrix and the actin cytoskeleton (14, 15). Signaling involves activation of Src and focal adhesion kinase (FAK)[1] and subse-

From the Departments of [a]Chemistry and Biochemistry and [e]Molecular, Cellular, and Developmental Biology and [c]Howard Hughes Medical Institute, University of Colorado, Boulder, Colorado 80309-0215, Departments of [g]Dermatology and [h]Medical Oncology, University of Colorado Health Sciences Center, Aurora, Colorado 80220, and [i]Department of Biochemistry and Molecular Biology, University of North Dakota, Grand Forks, North Dakota 58202

⌘ *Author's Choice*—Final version full access.

Received, April 6, 2009, and in revised form, July 14, 2009

Published, MCP Papers in Press, July 20, 2009, DOI 10.1074/mcp.M900178-MCP200

[1] The abbreviations used are: FAK, focal adhesion kinase; MRDI, mediator of RhoA-dependent invasion; RPMI, RPMI 1640 medium; FBS, fetal bovine serum; 2DE, two-dimensional electrophoresis; MTA, methylthioadenosine; *S*-AdoMet, *S*-adenosylmethionine; RNAi, RNA interference; shRNA, short hairpin RNA; CMV, cytomegalovirus; NCBInr, National Center for Biotechnology Information non-redundant; RPE, retinal pigment epithelial; N-WASP, neuronal Wiskott-Aldrich syndrome protein; 3D, three-dimensional; MTR-1-P, methylthioribose 1-phosphate; MTRu-1-P, methylthioribulose 1-phosphate; RBD, Rho binding domain of rhotekin; DN, dominant negative; WT, wild type; CM-DiIC$_{18}$, chloromethyl-1,1′-dioctadecyl-3,3,3′,3′-tetramethylindocarbocyanine perchlorate.

quent tyrosine phosphorylation of proteins recruited to integrin receptor complexes (16). Embryonic cells from $FAK^{-/-}$ mice lose motility and cannot be rescued with FAK harboring a Y397F autophosphorylation site mutation not because they fail to form focal adhesions but because they are unable to disassemble focal adhesions (17). Thus, Rho controls cell movement by modulating the turnover of focal adhesion complexes via FAK. However, the mechanisms by which Rho GTPases control FAK are incompletely understood.

In this study, we report that RhoA was constitutively activated in melanoma cells in a stage-specific pattern with elevated activity in cells from metastatic tumors. We present a functional proteomics screen for molecular targets of RhoA from which we identified a previously uncharacterized human protein induced in response to constitutive RhoA activation. This protein promoted Rho-dependent cell invasion and cell motility and provided a novel link for regulation of FAK tyrosine phosphorylation by RhoA. Thus, we refer to it as "mediator of Rho-dependent invasion (MRDI)." Although human MRDI has not been studied previously, it shows close sequence similarity to a methylthioribose-1-phosphate isomerase, which functions in methionine salvage pathways characterized in bacteria and yeast. We demonstrated that MRDI indeed has methylthioribose-1-phosphate isomerase activity and is required for methionine salvage in human cells. We further demonstrated that the catalytic activity of MRDI is independent of its role in cell invasion. Thus, MRDI is a dual function protein with promiscuous roles both as a metabolic enzyme and as an effector of signaling and cancer cell invasion.

MATERIALS AND METHODS

Cell Culture—Melanoma cell lines were obtained from ATCC or from Meenhard Herlyn (Wistar Institute) and maintained in 10% FBS, RPMI (18–22). Representative cell morphologies are shown in supplemental Fig. S2B. Human primary melanocyte cell lines (FOM71 and FOM78 from Dr. Herlyn; NHEM2493 and NHEM693 from BioWhittaker) were maintained in Medium 154 with melanocyte growth supplement (Cascade Biologics). At 70% confluence, cells were incubated for 24 h in 0.01% FBS, RPMI; then lysed; and extracted for two-dimensional electrophoresis (2DE). WM35 cells were also stably transfected with pMIG-RhoC (4) or control vector. Adenoviruses expressing constitutively active mutants RhoA-V14 or Rac1-V12 were prepared by recombination into the Ad5 genome using a β-galactosidase shuttle vector (23). Adenoviruses expressing dominant negative RhoA-N19 or Rac1-N17 were a gift from Joan Heller Brown (University of California San Diego). Infection was carried out at 10–20 plaque-forming units/cell for 24–48 h in 10% FBS, RPMI yielding >95% cell expression efficiency. In some cases cells were pretreated with Y27632 (30 μg/ml; Calbiochem), actinomycin (10 μg/ml; Sigma), cycloheximide (10 μg/ml; Sigma), C3 transferase (30 μg/ml), or lysophosphatidic acid (20 μM; Sigma). Transient transfection (90% efficiency) was obtained with FuGENE:cDNA (6:2) in retinal pigment epithelial cells (hTERT-RPE, Clontech) grown in 10% FBS, Dulbecco's modified Eagle's medium, F-12.

Vectors for Protein Expression and RNA Interference—MRDI was PCR-amplified from I.M.A.G.E. clone MGC3207 (Invitrogen) and subcloned into pCMV plasmid for expression in mammalian cells and into pMS356 plasmid for expression in *Escherichia coli*. His_6-MRDI was purified after isopropyl 1-thio-β-D-galactopyranoside induction in *E. coli* by nickel-nitrilotriacetic acid affinity chromatography and then treated with tobacco etch virus protease to remove the N-terminal His_6 tag. Proteins were stored at 3–4 mg/ml in 20 mM Tris, pH 8.0, 150 mM KCl, 5 mM 2-mercaptoethanol at −80 °C. A plasmid for bacterial expression of human methylthioadenosine phosphorylase (pQE32) was a kind gift from Drs. Indranil Basu and Vern Schramm (Albert Einstein College of Medicine). This was used to produce recombinant methylthioadenosine (MTA) phosphorylase purified by nickel-nitrilotriacetic acid affinity chromatography as described previously (24).

Double-stranded RNA interference (RNAi) oligonucleotides (200 pmol) were transfected into cells using DMRIE-C (1,2-dimyristyloxypropyl-3-dimethyl-hydroxyethylammonium bromide and cholesterol; Invitrogen). To inhibit RhoA or RhoC protein expression, cells were incubated for 48 h with oligonucleotide sequences (RhoA, 5′-GCAGGUAGAGUUGGCUUUGUU-3′; RhoC, 5′-GGAGAGAGCUGGCCAAGAUUU-3′), transfecting cells once at 0 h and again at 24 h. Cells were changed into medium containing 0.01% FBS, RPMI after the final transfection and then harvested at 48 h for Western blotting or applied to Matrigel assays for 24 h. To inhibit MRDI expression, cells were incubated for 48 h with four oligonucleotide sequences (1, 5′-GCAAGGAGATCATTATTGA-3′; 2, 5′-GCCAGGAGCTGACCGATGT-3′; 3, 5′-GCCCACCGCTGTCAACATG-3′; 4, 5′-GGATGGAACCCTAGATGGA-3′; Dharmacon) and then examined for phalloidin staining or Western blotting or applied to Matrigel assays for 24 h. Lamin A/C RNAi oligonucleotide (25) was used as a control.

Stable knockdown of MRDI was carried out in A375 cells by infection with lentivirus directing expression of green fluorescent protein and a U6 RNA promoter-driven shRNA-MRDI hairpin (FG12; Ref. 26) containing RNAi sequence 4. Stable transfectants were enriched by fluorescence-activated cell sorting using green fluorescent protein epifluorescence. MRDI-shRNA cells were then infected with retrovirus directing expression of MRDI containing five silent mutations (underlined) within the 19-bp shRNA sequence (5′-GGATGGCACATTGGACGGA-3′) generated by site-directed mutagenesis. MRDI-WT and active site mutations C168S (5′-GACTGTGCTGACCCACAGTAACACTGGTGCTC-3′) and D248A (5′-GGTCGTGGGAGCTGCCCGCGTGGTTGC-3′) containing silent mutations (underlined) were subcloned into the retroviral vector pREX for expression of CMV-MRDI and the extracellular domain of CD2. Stable knockdown and add-back expression cells were then enriched by fluorescence-activated cell sorting using anti-CD2-phycoerythrin (BD Pharmingen). Site-directed mutagenesis was carried out using the QuikChange site-directed mutagenesis system (Stratagene).

2DE and Mass Spectrometry—Cells were washed two times with PBS, extracted, and processed for isoelectric focusing as described previously (27) using Immobiline dry strips (pI 4–7, 18 cm; Amersham Biosciences) and 8–18% SDS-PAGE. Analytical (150 μg) or preparative (400 μg) gels were silver-stained using formaldehyde or methanol fixation, respectively (28, 29). Gels were analyzed with Melanie III (GeneBio), measuring protein intensities by percent volume (pixel intensities integrated over each area and divided by the sum of all intensities) and correcting each spot volume by subtracting a background volume of equal area. Changes were accepted when at least three gels from two independent experiments showed significant change in intensity by Student's t test ($p < 0.01$). Proteins were excised from wet gels, destained, digested in-gel with modified porcine trypsin (100 ng/digestion; Promega), and desalted on C_{18} ZipTips (Millipore). Peptides were cocrystallized with 2,5-dihydroxybenzoic acid on MALDI plates and analyzed using a Pulsar QqTOF mass spectrometer (Applied Biosystems). Peptide fingerprint spectra were summed over 50 acquisitions, and masses of the highest intensity peaks were matched against the NCBInr database (version

2005.01.06, 262,999 human/mouse entries) using MS-Fit. Searches specified trypsin cleavages with Cys-carbamidomethyl fixed and oxidized Met variable modifications allowing two missed cleavages, and peptide standards were used for external mass calibration. Details of results and excluded ions are listed in supplemental Table S1. At least two unique peptides in each digest were sequenced by MS/MS to confirm protein identifications where fragment peaks were chosen manually and searched against the NCBInr database using MS-Tag (supplemental Table S1). Mass tolerances of precursor and fragment ions were 0.1 Da. Each MS/MS spectrum was manually validated before acceptance.

Antibodies and Western Blotting—Cells were lysed in 50 mM Tris-HCl, pH 7.2, 2% SDS, 10 mM dithiothreitol, and protein concentration was determined using the DC assay (Bio-Rad). Extracts (30 μg) were separated by SDS-PAGE and transferred to PVDF membranes. Primary antibodies recognized RhoA (1:1000, mouse; ARH01, Cytoskeleton, Inc. or 1:1000, mouse; sc-13569(16C4), Santa Cruz Biotechnology, Inc.), RhoC (1:250, goat; sc-2648(G12), Santa Cruz Biotechnology, Inc.), γ-tubulin (1:1000, rabbit; sc-10732, Santa Cruz Biotechnology, Inc.), α-tubulin (1:1000, mouse; 3A2, Synaptic Systems), FAK-Tyr(P)^{397} (Westerns: 1:1500, rabbit; BIOSOURCE), FAK (1:1000, mouse; 610087, BD Transduction Laboratories), myosin phosphatase target subunit (MYPT1) (1:5000, rabbit; PRB-457C, Upstate), and MYPT1-Thr(P)^{696} (1:1000, rabbit; 07-251, Covance). Rabbit polyclonal antibodies were raised against a synthetic peptide corresponding to residues 356–369 of human MRDI (TISSRDGTLDGPQM; Sigma-Genosys) and used at 1:3000 dilution. Blots were probed with anti-mouse, anti-rabbit (Jackson ImmunoResearch Laboratories), or anti-goat (Calbiochem) secondary antibody (1:10,000) coupled to horseradish peroxidase and visualized by enhanced chemiluminescence (Amersham Biosciences). Intensities were quantified using ImageJ software (30).

Microscopy—Indirect immunofluorescence was carried out on A375 cells fixed and permeabilized with 0.1% glutaraldehyde, PBS and 0.1% Triton X-100, PBS and on retinal pigment epithelial (RPE) cells fixed and permeabilized with 4% formalin (Sigma) and 0.1% Triton X-100, PBS. Coverslips were blocked with 5% BSA and incubated with anti-MRDI (1:1000), anti-neuronal Wiskott-Aldrich syndrome protein (N-WASP) (1:200, goat; sc-10122(D15), Santa Cruz Biotechnology, Inc.), anti-vinculin (1:500, mouse; HVIN-1, Sigma), anti-FAK-Tyr(P)^{397} (1:500, mouse; BD Transduction Laboratories), or anti-paxillin-Tyr(P)^{118} (1:500, mouse; BD Transduction Laboratories) followed by secondary antibodies coupled to Alexa Fluor 488 or Alexa Fluor 592 (Molecular Probes). For F-actin staining, cells fixed with 4% formalin were incubated with rhodamine phalloidin (3.3 nM; Molecular Probes). Membrane staining was carried out using CellTracker CM-DiIC$_{18}$ (1 μg/ml; Molecular Probes) as a fluorescent lipophilic marker. Cells were monitored with a Zeiss Axioplan II fluorescence microscope outfitted with an apochromatic lens with a high numerical aperture (1.4) and a corrective lens element for spherical aberrations. The *z* axis resolution of this instrument is ~400 nm. Data were collected using a Cooke SensiCam charge-coupled device camera and SlideBook software (Intelligent Imaging Innovations).

Live cell imaging was performed on an Olympus IX81 inverted microscope equipped with a heated stage. Images were acquired with an ORCA-100 digital camera (Hamamatsu) and analyzed with Slidebook software. Cells were grown on collagen-coated coverslips in RPMI, 10% FBS and serum-starved for 1 h. Serum was added to a final concentration of 10%, and cells were monitored for 60 min. ImageJ was used to track cells *versus* time.

Immunohistochemistry—Sections from formalin-fixed, paraffin-embedded patient biopsies were deparaffinized, rehydrated, and treated with antigen retrieval solution (Dako Cytomation) in a decloaking chamber (Biocare Medical) first at 120 °C for 30 s and then at 85 °C for 10 s. Sections were stained with anti-MRDI (1:200 overnight followed by anti-rabbit horseradish peroxidase and developed with 3,3′-diaminobenzidine (Dako Cytomation Envision Elite). Specimens were then counterstained with hematoxylin and azure B (Sigma). Negative controls with antibody preincubated with 0.1 mg/ml peptide were used to verify low background staining. A tissue microarray (YMTA 33, Yale tissue microarray facility, Yale University, New Haven, CT) containing 200 specimens, including melanomas from organs other than skin, was processed in a similar manner. Xenograft tissues were prepared by injecting A375 cells (10^6 cells) intradermally to the right posterior flank of female NIH athymic nu/nu mice. After 6 weeks, mice were sacrificed by cervical dislocation, and tumors were dissected, fixed in formalin, embedded, and processed for immunohistochemistry with anti-MRDI + diaminobenzidine.

Cell Invasion—Cells were transfected with RNAi oligonucleotide to suppress MRDI protein expression, and 5×10^4 cells were plated onto upper chambers of a Matrigel assay system (24-well; BD Biosciences) using serum-free RPMI in upper chambers and 10% FBS, RPMI in lower chambers. After 24 h, invaded cells on the lower chamber membrane surfaces were fixed, visualized with Wright-Giemsa stain (Sigma), and counted. Spheroid assays were carried out as described by Smalley *et al.* (45). Melanoma cells were plated on 1.5% Noble agar for 3–5 days. Spheroids were collected and centrifuged (3000 rpm) to remove medium; gently resuspended in 2.5 mg/ml bovine dermal collagen (PureCol, INAMED, Leimuiden, Netherlands) in RPMI, 10% FBS; and overlaid on a presolidified layer of the same collagen solution. The collagen/cell suspension was allowed to solidify for 1 h and then overlaid with RPMI, 10% FBS. Spheroids were grown for 10 days after implanting to monitor 3D growth and invasion into collagen, and images were collected by phase microscopy.

Enzyme Assays—Methylthioribose 1-phosphate (MTR-1-P) was produced by incubating 1 mM MTA with methylthioadenosine phosphorylase (1 μM) in 100 mM NaP_i, pH 7.4, 0.5 mM DTT, 0.5 mM EDTA for 16.5 h at 37 °C. Reactions were conducted in the presence or absence of purified MRDI (1 μM) to assay conversion of MTR-1-P to methylthioribulose 1-phosphate (MTRu-1-P). Reactions were clarified by ultrafiltration to remove proteins, and reaction products were examined by ^{1}H NMR (Varian 600-MHz spectrometer). Chemical shift assignments were matched to those described for purified MTR-1-P and MTRu-1-P by Furfine and Abeles (31).

Rho GTPase Assays—Rho-GTP was assayed by adapting published protocols (32) to reduce background and enhance signal to noise. Proteins were extracted for 3 min at 4 °C in lysis buffer (50 mM Tris-HCl, pH 7.5, 1% Triton X-100, 0.5% sodium deoxycholate, 0.1% SDS, 0.65 M NaCl, 10 mM $MgCl_2$, 10 μg/ml leupeptin, 10 μg/ml aprotinin, 1 mM PMSF; 0.7 ml). Clarified extracts were incubated for 20 min at 4 °C with glutathione-Sepharose (Amersham Biosciences) coupled to bacterially expressed GST-RBD (Rho binding domain of rhotekin; 30 μg) and then washed five times with lysis buffer. Samples precipitated from 200 μg of total protein were resolved by 12.5% SDS-PAGE, and bound RhoA-GTP and RhoC-GTP were visualized by Western blotting with anti-RhoA or -RhoC antibodies.

RESULTS

Stage-specific Activation of RhoA in Melanoma Cell Lines—We monitored the activation of RhoA in 20 melanocyte or melanoma cell lines cultured from radial growth phase, vertical growth phase, or metastatic tumors that had been catalogued with respect to tumor pathology, tumorigenicity, and soft agar growth (18–21). The activity state of RhoA from cell lysates was measured by GTP binding and subsequent association with GST-RBD. The highest frequency of acti-

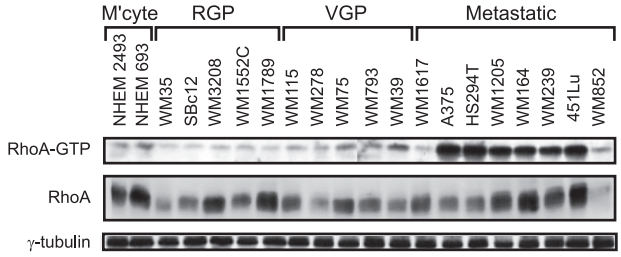

FIG. 1. **Stage-specific activation of RhoA in melanoma cells.** RhoA activation was measured by Rho-GTP binding to GST-RBD. Western blots show levels of RhoA-GTP bound to GST-RBD in pull-down assays and RhoA and γ-tubulin in total cell lysates. Similar results were observed in three independent experiments. *RGP*, radial growth phase; *VGP*, vertical growth phase; *M'cyte*, melanocyte.

vated RhoA was observed in cells of metastatic origin where six of eight metastatic cell lines showed elevated RhoA-GTP in a manner uncorrelated with total RhoA expression (Fig. 1). Enhanced specific activity was verified by normalizing RhoA-GTP signal to total RhoA protein (supplemental Fig. S1). The results indicate that RhoA is activated in cells derived from human metastatic melanomas.

A Functional Proteomics Screen for RhoA Pathway Targets—To identify targets downstream of RhoA, constitutively active mutant RhoA-V14 was expressed by adenoviral delivery into WM35, an early stage nonmetastatic cell line derived from a primary superficial spreading melanoma from a patient with no metastasis (18). WM35 cells grow slowly, form few colonies in soft agar, and do not form tumors in nude mice. Proteins in soluble lysates were resolved by 2DE and visualized by silver staining, monitoring proteins whose intensities changed reproducibly by >1.5-fold following RhoA-V14 expression compared with control cells infected with empty adenovirus. The expression of RhoA-V14 led to cell contraction and rounding (supplemental Fig. S2A). Five proteins showing features that were reproducibly altered in response to RhoA were identified by in-gel digestion followed by peptide mass mapping and peptide sequencing by mass spectrometry (supplemental Table S1). Of these, two (tropomyosin and protein phosphatase 1B) were characterized previously as downstream targets of RhoA signaling (33–36). Thus, three novel cellular targets of RhoA signaling were identified by the screen.

We next asked which of these proteins were functional RhoA targets during melanoma progression. We hypothesized that proteins that were functional mediators of RhoA signaling would be regulated across many cell lines in a manner correlating with the activation state of RhoA. The five proteins found to be responsive to RhoA were examined by 2DE in 14 melanocyte and melanoma cell lines, comparing their signal intensities with those in unstimulated WM35 cells (Fig. 2*A*). Only three of the proteins responsive to RhoA in WM35 cells showed 2DE signals in other melanoma cell lines, and of these, only one showed increased intensity in metastatic cells consistent with the pattern of RhoA activation (supplemental Fig. S3). MGC3207 is a previously uncharacterized gene annotated as a human "hypothetical protein" (Fig. 2*B*). Intensities of features from MGC3207 were elevated in WM35 cells stimulated with RhoA and in metastatic lines (A375, HS294T, and Lu451) compared with unstimulated WM35 cells (Fig. 2*C*) commensurate with a potential change in protein expression. We hypothesized that MGC3207 might function to regulate RhoA signaling responses important for metastatic cell behavior. Based on its characterization below, we refer to this protein throughout as MRDI.

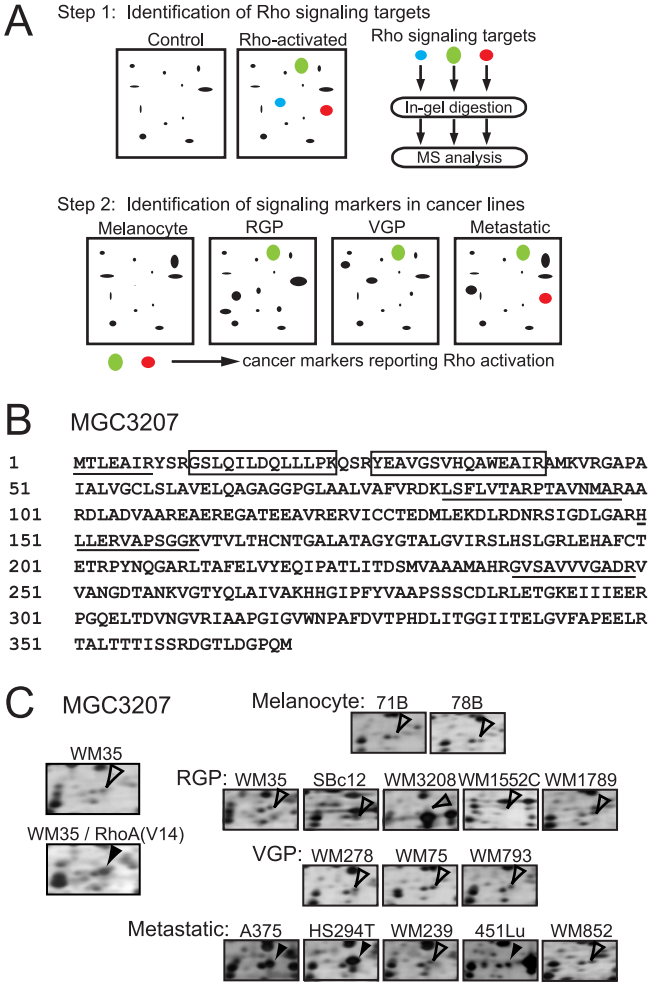

FIG. 2. **A functional proteomics screen for RhoA targets.** *A*, outline of the experimental strategy for identifying proteins responsive to RhoA. *Step 1*, protein responses to RhoA-V14 are profiled in WM35 cells by 2DE to identify pathway targets. *Step 2*, these targets are examined in other melanoma cell lines to identify those that correlate with RhoA activation. *B*, sequence of human MGC3207 indicating peptides observed by peptide mass matching (*underlined*) or MS/MS sequencing (*boxed*). *C*, 2DE images showing MGC3207 protein changes responsive to RhoA in WM35 cells and across melanocyte and melanoma cell lines. *Arrowheads* show protein intensities that are unaltered (*open*) or altered in the same direction as those induced by RhoA signaling (*closed*). *RGP*, radial growth phase; *VGP*, vertical growth phase.

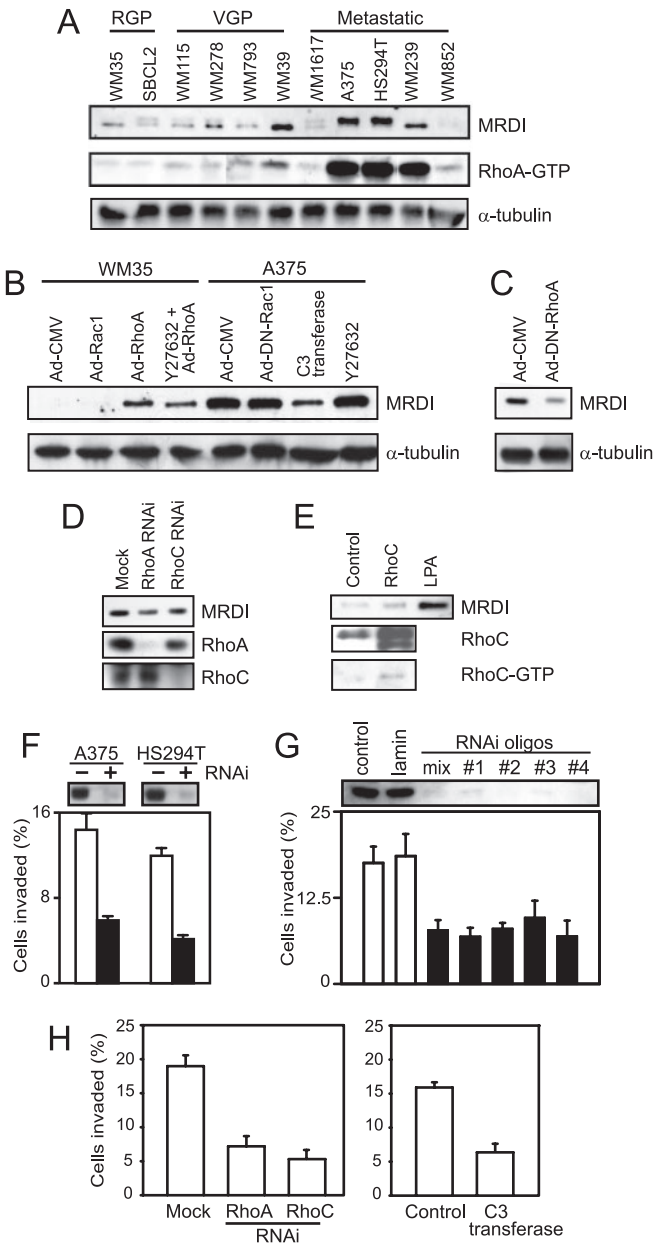

FIG. 3. **MRDI is induced by RhoA and mediates RhoA-dependent cell invasion.** *A–E*, Western blots demonstrate that RhoA induces expression of MRDI. *A*, blots probed with anti-MRDI show elevated protein levels in metastatic cell lines with constitutive RhoA activity. RhoA-GTP blots are from the image in Fig. 1*A*. Loading controls show α-tubulin in total lysates. *B*, RhoA is necessary for MRDI induction. Extracts (5 μg) were probed with anti-MRDI, examining WM35 cells treated by adenoviral delivery of Ad-CMV, Ad-Rac1-V12, or Ad-RhoA-V14 or pretreated with Y27632 prior to Ad-RhoA-V14 (*lanes 1–4*). A375 cells were treated with Ad-CMV, Ad-DN-Rac1, C3 transferase, or Y27632 (*lanes 5–8*). *C*, A375 cells were treated with Ad-CMV or Ad-DN-RhoA-N19, and lysates were blotted with anti-MRDI. *D*, A375 cells were treated with RNAi for 48 h to inhibit expression of RhoA or RhoC, and lysates were blotted with anti-MRDI. Anti-RhoA or anti-RhoC Westerns demonstrate selective knockdown by RNAi. *E*, control or RhoC-expressing WM35 cells were examined for expression of MRDI and RhoC, and RhoC-GTP was assayed by GST-rhotekin pulldown assays. RhoC overexpression and activation had little effect on MRDI compared with cells treated with lysophosphatidic acid (*LPA*) (24 h). *F–H*, MRDI promotes cell invasion. *F*, RNAi knockdown of MRDI in metastatic melanoma A375 and HS294T cells inhibits cell invasion through Matrigel. *G*, invasion is suppressed in A375 cells treated with four different MRDI-RNAi oligonucleotide sequences, singly or in combination, but not in cells treated with lamin A/C-RNAi (48-h transfection). Values represent mean ± S.D. ($n = 3$). *H*, cell invasion depends on Rho signaling. Invasion is reduced in A375 cells treated with RhoA-RNAi, RhoC-RNAi, or C3 transferase. *RGP*, radial growth phase; *VGP*, vertical growth phase.

MRDI Is Induced by Constitutive RhoA Signaling—Peptide antibodies were produced to characterize MRDI expression. Western blotting confirmed that expression of the expected 40-kDa protein was elevated in metastatic lines in a manner that correlated with RhoA activation (Fig. 3*A*). MRDI showed variable gel mobility in different lines; we ascribed this to differences in covalent modification because 2DE blots showed that MRDI separated into three spots with similar mass and varying pI, indicating the existence of at least two post-translationally modified forms (supplemental Fig. S4A). However, all forms were increased in response to RhoA, and we were unable to detect evidence for regulated covalent modification.

MRDI protein expression was elevated in premetastatic (WM35) cells expressing RhoA-V14 but not Rac-V12, indicating its selective response to RhoA (Fig. 3*B*). Its expression in metastatic (A375) cells was reduced by inhibiting RhoA-GTP with C3 transferase or dominant negative (DN) RhoA-N19 (Fig. 3, *B* and *C*). Likewise RhoA knockdown by RNAi resulted in partial inhibition of MRDI expression (Fig. 3*D*), although because cell viability was compromised by RhoA-RNAi, the experiment could not be carried out long enough for complete protein turnover. Taken together, the results demonstrate that RhoA activation is necessary for elevated MRDI expression. Induction of MRDI was blocked by inhibiting transcription with actinomycin D or inhibiting protein synthesis with cycloheximide, indicating that RhoA-dependent expression is most likely regulated transcriptionally (supplemental Fig. S4B).

We next examined MRDI expression in WM35 cells stably transfected with RhoC. RhoC overexpression in melanoma cell lines enhances morphological transformation, cell survival, and cell invasion (4, 37). However, RhoC led to little or no induction of MRDI under conditions where GTP loading was confirmed by GST-rhotekin pulldown assays (Fig. 3*E*). Selective knockdown of RhoC by RNAi resulted in little suppression of MRDI (Fig. 3*D*). We conclude that MRDI is primarily induced by RhoA and less responsive to RhoC in nonmetastatic and metastatic cells. Pretreating cells with the Rho-activated kinase inhibitor Y27632 did not alter RhoA-dependent induction of MRDI (Fig. 3*B*), indicating that its expression is not regulated by the RhoA-Rho-activated kinase branch point. Positive controls confirmed that Y27632 inhib-

ited Rho kinase activity *in vitro* and suppressed Rho signaling in melanoma cells (supplemental Fig. S5).

MRDI Promotes Cell Invasion—We next assayed cell invasion through Matrigel and observed significant repression of invasion in metastatic cell lines (A375 and HS294T) when MRDI expression was inhibited with RNAi (Fig. 3*F*). The specificity of inhibition was confirmed by four different MRDI-RNAi oligonucleotides with no effect using lamin A/C-RNAi as a negative control (Fig. 3*G*). Invasion was also repressed by MRDI knockdown in metastatic WM239A cells but was unaffected in nonmetastatic cells in which MRDI expression was normally low (supplemental Fig. S6). RNAi knockdown of either RhoA or RhoC or treatment of cells with C3 transferase also caused repression of invasion (Fig. 3*H*). The results show that Rho promotes invasion in metastatic melanoma cell lines and indicate that MRDI mediates Rho signaling to cell invasion. Thus, MRDI is a functional target of RhoA, which controls downstream responses to this pathway.

Cytoplasmic and Membrane Localization of MRDI in Human Melanomas—Examination of human melanoma specimens revealed correlations between tumor stage and subcellular localization of MRDI. Biopsies of atypical/dysplastic nevi, primary melanomas, and metastatic melanomas were immunostained with anti-MRDI antibody, counterstained with hematoxylin-azure B, and observed by light microscopy. MRDI immunoreactivity was observed within cells of melanocyte origin, keratinocytes, endothelial cells, and infiltrating lymphocytes. Importantly the immunoreactivity in nontumorigenic melanocytes located within atypical or dysplastic nevi was mostly nuclear and often accentuated at nuclear membranes (Fig. 4*A* and supplemental Fig. S7A). In contrast, primary and metastatic melanomas within skin often showed elevated MRDI immunoreactivity in cytoplasmic compartments (Fig. 4*B* and supplemental Fig. S7B). Immunoreactivity was also examined in metastatic tumors taken from lymph node and other non-skin tissues. Although the intensity of immunostaining was variable in these samples, metastatic melanomas generally showed higher MRDI localization within cytoplasmic compartments compared with early stage melanomas (supplemental Fig. S7C). Antibody specificity was confirmed by peptide competition controls (supplemental Fig. S7D). Together the results suggest that cytoplasmic pools of MRDI increase whereas nuclear pools decrease during advanced stages of disease.

Interestingly MRDI immunoreactivity within primary and metastatic tumors was often observed to be accentuated at membrane regions where cells contacted each other (Fig. 4*B*, *inset*, *arrowheads*). Similar patterns were observed in xenograft tissues grown by subcutaneous injection of metastatic A375 cells into immunodeficient mice (Fig. 4*C*, *arrowheads*). Consistent with this, immunocytochemistry of cultured A375 cells showed that MRDI localized to membrane protrusions at the cell periphery as well as within the cell body (Fig. 4*D*). All of the reactivity at cell protrusions but only part of the cell body reactivity was reduced upon blocking MRDI expression by RNAi (Fig. 4*D*) with similar effects observed using peptide competition (data not shown), suggesting that nuclear staining partly reflects nonspecific reactivity.

Similar results were observed upon transient expression of MRDI into non-melanoma cells that express low amounts of protein endogenously. Immunostaining of RPE cells showed transfected MRDI at the membrane leading edge, colocalizing with the fluorescent membrane tracer CM-DiIC$_{18}$ (Fig. 4*E*). In addition, MRDI colocalized with N-WASP (Fig. 4*F* and supplemental Fig. S8), a ubiquitous adaptor protein that mediates agonist-induced F-actin nucleation and polymerization by binding Arp2/3 (38). No overlap was observed between MRDI and actin stress fibers or the focal adhesion markers vinculin, FAK, and paxillin (supplemental Fig. S8). Thus, the cellular localization of MRDI reflects membrane accentuation in melanoma cells in both tissues and cultured cells.

MRDI Promotes Cell Movement and Tyrosine Phosphorylation of Focal Adhesion Kinase—Given its function in cell invasion, the membrane localization of MRDI suggested potential control of events involved in cell motility and/or cell-substrate interactions. Therefore, cells from a metastatic tumor (A375) were examined by live cell imaging before and after knockdown of MRDI by RNAi, and cell motility was monitored by tracking nuclear movement for 60 min. Whereas control cells showed elevated motility following serum stimulation, cells in which MRDI was inhibited became flatter after serum addition and showed significantly reduced movement (Fig. 5*A* and supplemental Movies S1 and S2). Scoring cells across several experiments, MRDI knockdown caused a 2-fold decrease in the number of cells that migrated by more than one nuclear diameter in 60 min ($\sim$25 μm/h) and a 2.8-fold decrease in cells migrating by more than two nuclear diameters ($\sim$50 μm/h) compared with controls.

Finally we examined the influence of MRDI on biochemical events regulated by RhoA. In a nonmetastatic melanoma cell line in which the activity of RhoA is normally low (WM35) expression of RhoA-V14 caused elevated tyrosine phosphorylation of FAK at Tyr^{397} (Fig. 5*B*). Moreover in a metastatic cell line in which RhoA is normally activated (A375), FAK-Tyr(P)^{397} was constitutively high and was reduced upon inhibiting RhoA with C3 transferase. Importantly inhibiting MRDI expression by RNAi eliminated FAK-Tyr(P)^{397} in metastatic cells. This demonstrates that FAK autophosphorylation is RhoA-dependent and that MRDI is required for this regulation. Previous studies have shown that cells from FAK$^{-/-}$ mice lose motility and cannot be rescued with mutant FAK-Y397F because they fail to disassemble focal adhesion complexes (14). We therefore hypothesized that MRDI might enhance focal adhesion turnover, which would repress stress fiber formation. We examined this prediction and found that knockdown of MRDI in cells from a metastatic tumor caused a significant increase in actin stress fibers compared with controls (Fig. 5*C*). Taken together, the results suggest that MRDI promotes

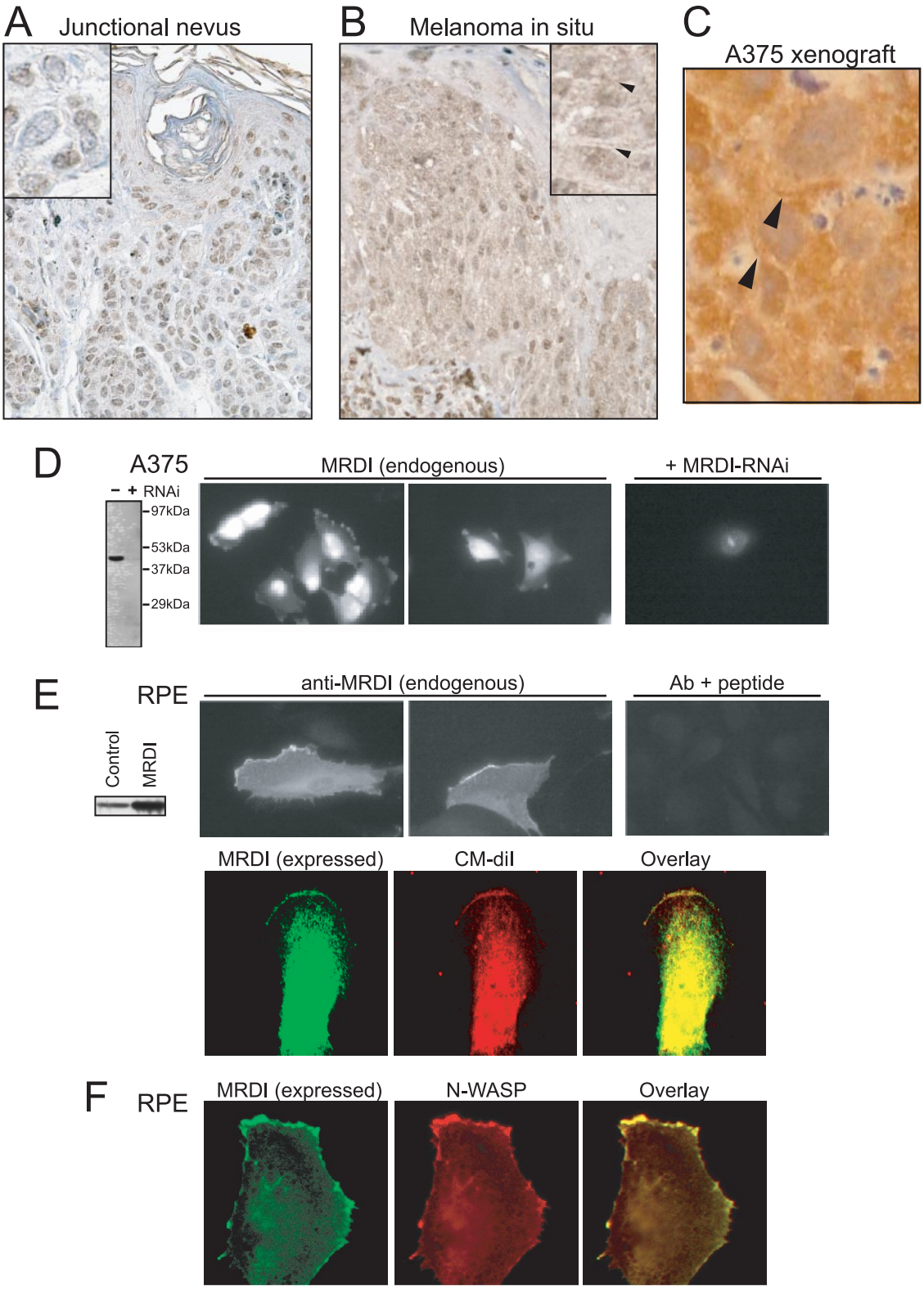

FIG. 4. **MRDI localizes to membranes and cell protrusions.** *A* and *B*, MRDI localization correlates with tumor grade in human melanoma specimens. *A*, junctional compound nevus shows nuclear localization but little cytoplasmic immunoreactivity. *B*, melanoma *in situ* shows MRDI immunoreactivity localized to cytoplasmic pools. The *inset* at higher magnification illustrates membrane accentuation of immunoreactivity (*arrowheads*). *C*, MRDI immunostaining shows membrane accentuation between cells in xenograft tumors of A375 cells grown in athymic nude mice (*arrowheads*). *D*, MRDI localizes to cell protrusions in cultured A375 cells when probing endogenous MRDI with anti-MRDI (1:3000). Cells

cell invasion in response to constitutive RhoA activation in part by promoting FAK tyrosine phosphorylation and stress fiber turnover.

MRDI Has Dual Function as a Metabolic Enzyme—MRDI has never been characterized in human systems and in the human database is often annotated as a hypothetical protein. Sequence alignments showed that MRDI belongs to a protein family of translational initiation factors, sharing a motif of 25 residues (residues 322–346) with α, β, and δ subunits of the guanine nucleotide exchange factor eIF2B (39). However, this association yielded little insight into protein function because exchange factor activity is catalyzed by the γ/ε subunits of eIF2B, whereas the functions of the $\alpha/\beta/\delta$ subunits are unknown. Further examination showed that a subset of this family contains genes unrelated to translational initiation that instead function in amino acid salvage (supplemental Fig. S9). During polyamine synthesis, decarboxylated *S*-adenosylmethionine (*S*-AdoMet) is converted to MTA, which cannot be converted back to *S*-AdoMet and must instead be catabolized to its end product, methionine (40). Thus, the pathway of MTA catabolism results in methionine salvage (Fig. 6*A*). Human MRDI appears to be an ortholog of enzymes characterized in *Bacillus subtilis*, *Klebsiella pneumoniae*, and *Saccharomyces cerevisiae* that catalyze the isomerization of MTR-1-P to MTRu-1-P (41–43). This suggested that MRDI might serve as an isomerase in the human methionine salvage pathway, which has never been fully elucidated.

To test this hypothesis, MTR-1-P was produced enzymatically from MTA using purified MTA phosphorylase. ^{1}H NMR confirmed the presence of MTR-1-P by matching chemical shift peaks to those assigned previously (31) (Fig. 6*B*). Incubation of MTR-1-P with purified recombinant MRDI led to the reduction of substrate peak intensities and the new appearance of peaks assigned previously to MTRu-1-P (Fig. 6*C*). This confirmed that MRDI has enzymatic activity as a MTR-1-P isomerase in catalyzing the *in vitro* conversion of the substrate, MTR-1-P, to its product, MTRu-1-P.

Previous x-ray structure determinations of MTR-1-P isomerase from *B. subtilis* and *S. cerevisiae* each revealed a homodimer of 40-kDa subunits (43, 44). The *S. cerevisiae* structure (Protein Data Bank code 1W2W; Ref. 43) showed well ordered sulfate ions present at the interface between two domains in each monomer that were proposed to occupy the binding site for the phosphate moiety of MTR-1-P in the enzyme active site (supplemental Fig. S10A). The *B. subtilis* structure confirmed cocrystallization of the product, MTRu-1-P, within this site (Protein Data Bank code 2YRF; Ref. 44). The residues coordinating the sulfate ion form an interface between solvent and a deep hydrophobic pocket containing Asp and Cys residues that are conserved throughout the subfamily and correspond to Cys^{168} and Asp^{248} in human MRDI (supplemental Fig. S10B). We therefore constructed the mutations C168S and D248A in human MRDI and tested their effects on *in vitro* isomerase activity. Either mutation inhibited turnover of MTR-1-P to MTRu-1-P (Fig. 6, *D* and *E*). This identified Cys^{168} and Asp^{248} as active site residues required for MTR-1-P isomerase catalytic activity.

To test the cellular function of MRDI in methionine salvage, we measured the dependence of cell growth on MTA. Cells incubated in medium lacking methionine failed to grow, consistent with a requirement for this essential amino acid in human cells (Fig. 7*A*). In contrast, methionine-free medium supplemented with MTA supported cell growth to levels reaching 25% of that in full medium (Fig. 7*A* and supplemental Fig. S11). Importantly stable knockdown of MRDI completely prevented cell growth in the presence of MTA, and the phenotype was rescued by stable expression of MRDI-WT harboring silent mutations to bypass the shRNA knockdown (Fig. 7, *A* and *B*). In contrast, expression of MRDI-C168S or -D248A mutants failed to rescue the growth phenotype (Fig. 7*B*). This confirms that MTA is a precursor of methionine in human cells and that the catalytic activity of MRDI as an MTR-1-P isomerase is necessary for metabolic flux through the methionine salvage pathway.

Finally we asked whether the catalytic function of MRDI is relevant to its role in cell invasion. A375 cells were grown as spheroid colonies embedded in collagen, an assay that mimics 3D growth and invasion by melanoma cells surrounded by the main extracellular matrix protein found in human dermis (45). Knockdown of endogenous MRDI had no effect on spheroid growth rate but significantly blocked cell invasion into collagen (Fig. 7, *C* and *D*). Expression of MRDI-WT in the stable knockdown cells rescued the cell invasion phenotype, confirming the specificity of the shRNA response (Fig. 7, *E* and *F*). The key finding was that neither C168S nor D248A mutations affected the ability of MRDI to rescue the knockdown phenotype (Fig. 7, *G* and *H*). The results confirm that MRDI promotes melanoma cell invasion in 3D culture and demonstrates that its catalytic activity as an isomerase is not necessary for its function in RhoA signaling and invasion.

DISCUSSION

Our study provides novel insights into how the RhoA pathway controls the cancer phenotype of cell invasion. In melanoma cell lines, MRDI represents a novel target of Rho signaling, functioned in cell invasion, and was necessary for

treated with MRDI-RNAi show loss of reactivity at the membrane leading edge and protrusions and partial loss of nuclear staining. Western blots of lysates (5 μg) probed with anti-MRDI confirm knockdown (*left panel*). *E*, RPE cells transfected with MRDI or empty vector and probed with anti-MRDI antibody (*Ab*) and CM-DiIC$_{18}$ (*CM-dil*) show localization of MRDI at the membrane periphery and leading edge. Western blots of lysates (20 μg) show low protein expression in untransfected cells and elevated expression upon transfection (*left panel*). *F*, indirect immunofluorescence of RPE cells shows colocalization of MRDI with N-WASP at the membrane leading edge.

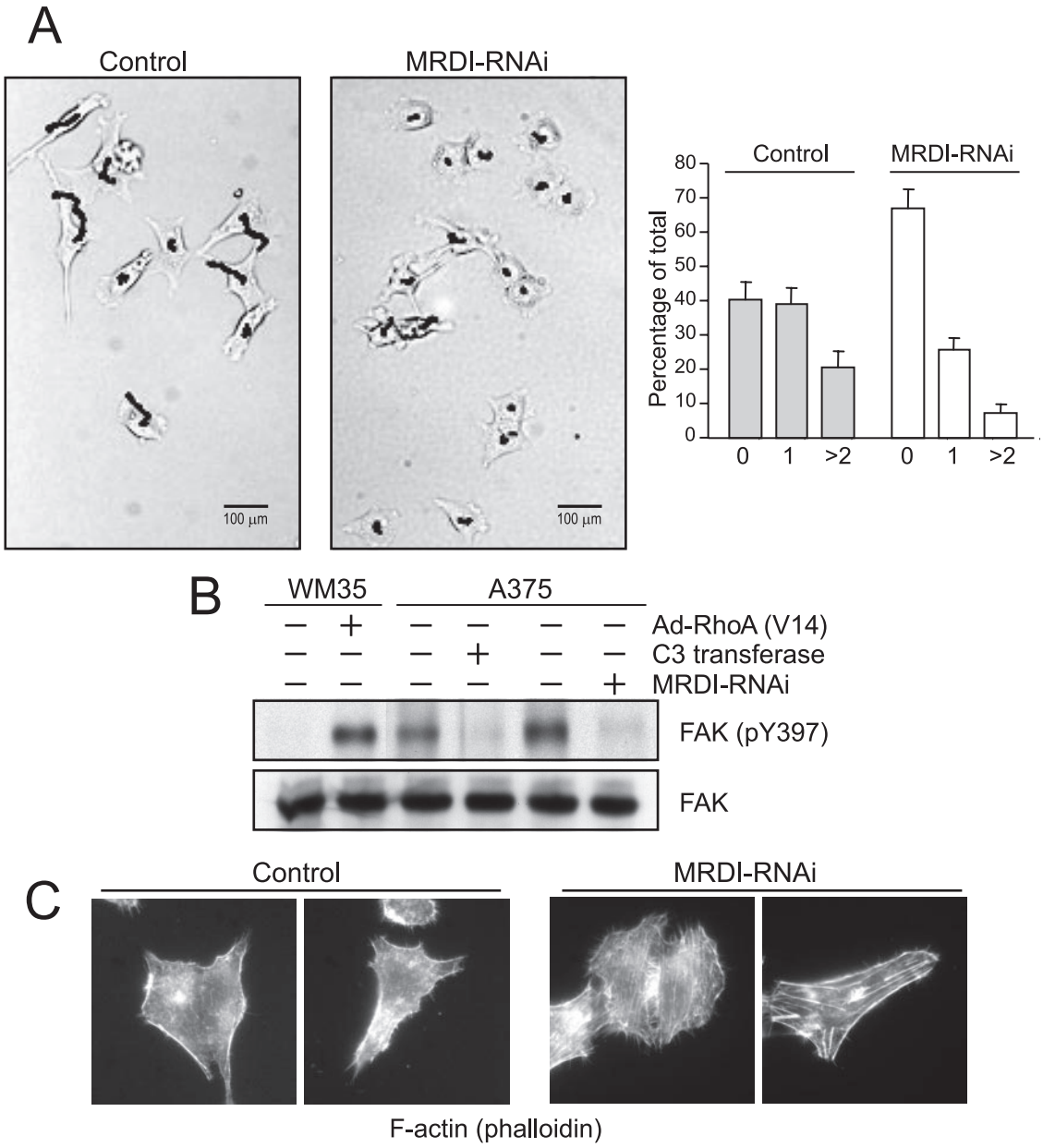

FIG. 5. **MRDI modulates cell motility, FAK phosphorylation, and stress fiber formation.** *A*, live cell images of A375 cells treated with control scrambled oligonucleotide or MRDI-RNAi show decreased cell movement following MRDI knockdown. Images are taken at $t = 0$ after serum addition, and traces show nuclear movement over the next 60 min. *Right panel*, summary of several biological replicates quantifying percentages of control and MRDI-RNAi cells that move by less than one ("*0*"), between one and two ("*1*"), and more than two ("*2*") nuclear diameters in 60 min. Values show mean ± S.E. (number of experiments, $n = 9$ control and $n = 8$ RNAi). *B*, FAK-Tyr(P)^{397} is up-regulated in WM35 cells expressing Ad-RhoA-V14 (*lanes 1* and *2*) and inhibited in A375 cells treated with C3 transferase (*lanes 3* and *4*) or MRDI-RNAi (*lanes 5* and *6*). In contrast, total FAK protein expression is unaffected. *C*, MRDI knockdown enhances actin polymerization. A375 cells were transfected for 48 h with or without MRDI-RNAi and observed following phalloidin staining. Two representative cells are shown in each experiment.

autophosphorylation of FAK, a key mediator of focal adhesion turnover. MRDI showed targeting to membranes in advanced human melanoma specimens and localizes at the leading edge of cells in culture. A role in regulating membrane events was also suggested in cultured cells by live cell imaging and findings that link MRDI to FAK phosphorylation and stress fiber destabilization consistent with its role in promoting cell invasion. Taken together, our results suggest that MRDI promotes cell invasion under conditions of RhoA pathway dysregulation by regulating molecular events key to the control of membrane dynamics and cell adhesion. A working model is presented in supplemental Fig. S12.

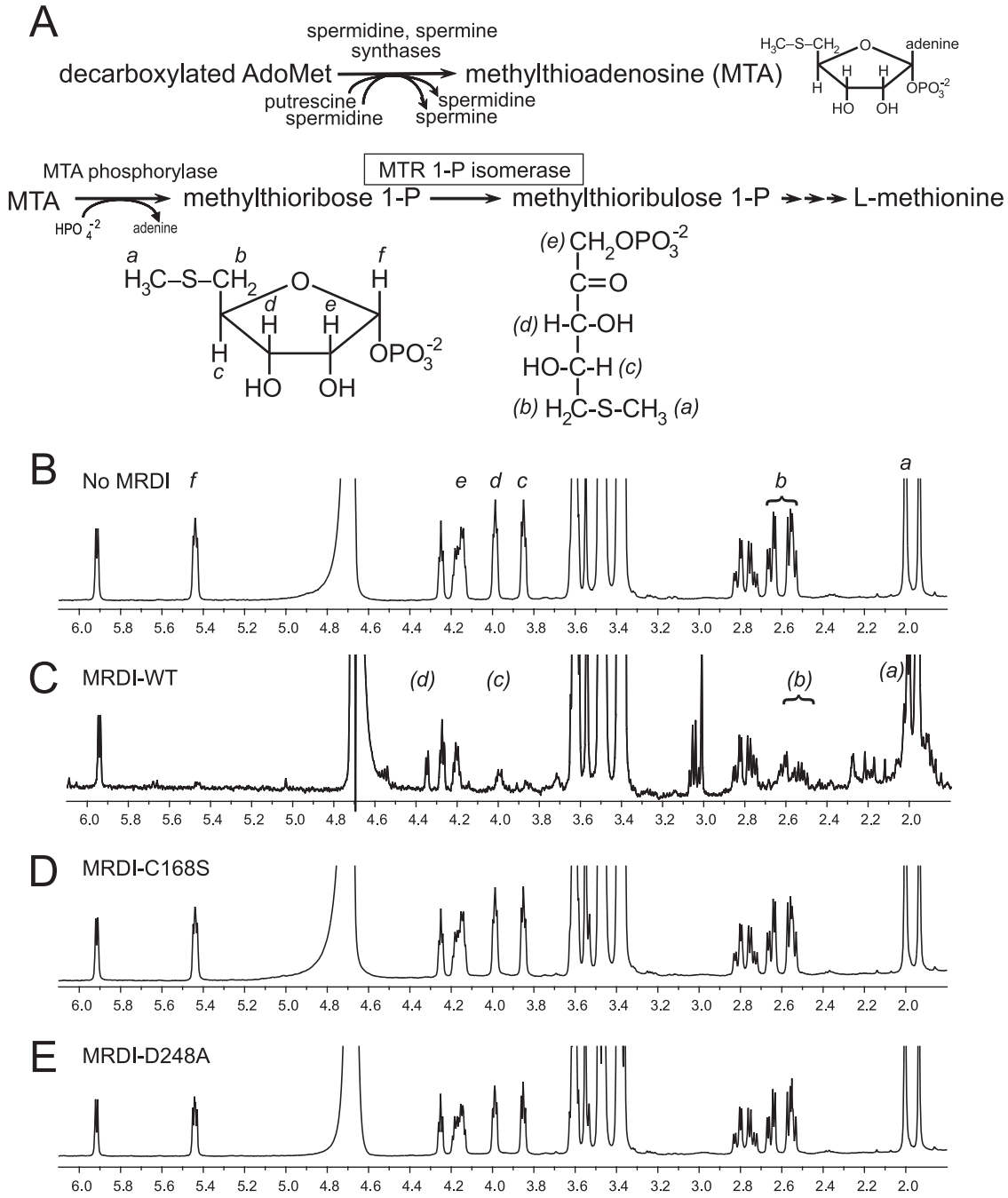

FIG. 6. **MRDI is a methylthioribose-1-phosphate isomerase.** *A*, enzymatic steps in the methionine salvage pathway. Following conversion of decarboxylated *S*-AdoMet to MTA during polyamine synthesis, MTA is catabolized to methionine. *B–E*, recombinant purified MRDI shows MTR-1-P isomerase enzymatic activity. ^{1}H NMR spectra, collected after *in vitro* reactions in the absence (*B*) or presence (*C*) of wild type MRDI, show that MRDI catalyzes the conversion of MTR-1-P to MTRu-1-P. In contrast, catalytic turnover is absent in reactions with MRDI-C168S (*D*) or MRDI-D248A (*E*) mutants. Peak assignments (*a–f*) in *B* and *C* correspond to protons indicated in *A*.

Our proteomics screening strategy involved profiling protein responses to RhoA activation in cells in which the pathway was normally "off" and then carrying out a second screen to filter for targets uniformly regulated across cell lines in which RhoA was constitutively "on." Only one of the five RhoA targets identified initially in premetastatic cells turned out to be highly correlated with constitutive RhoA activation across many cell lines. The fact that MRDI was validated as a regulator of RhoA-dependent cellular responses and correlated with melanoma stage illustrates the utility of prioritizing functional targets by filtering out bystanders that vary between cells because they have no regulatory function.

Our study also showed that the activation state of RhoA is differentially elevated in melanoma cell lines derived from

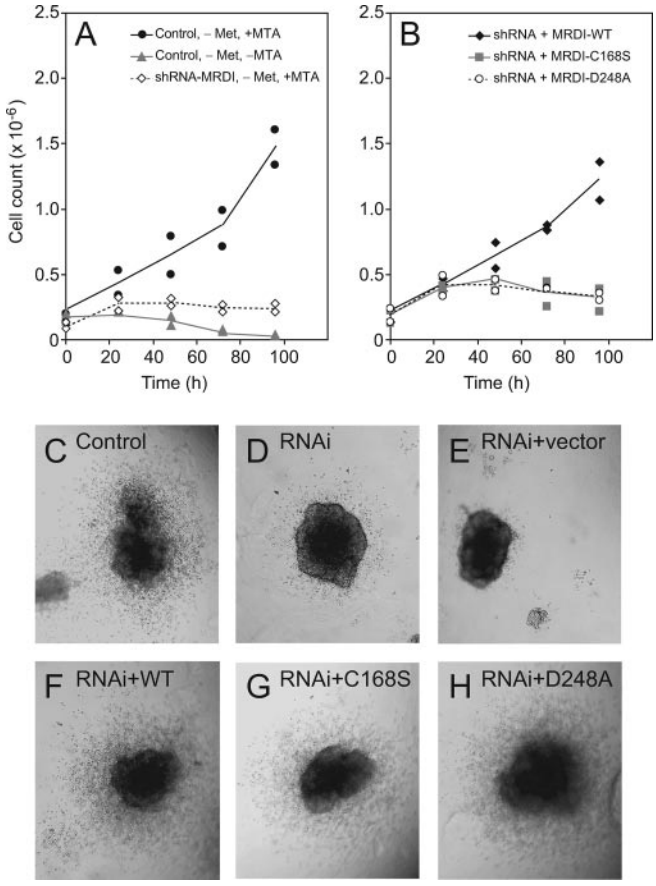

FIG. 7. **Catalytic activity of MRDI is required for methionine salvage but not cell invasion.** *A*, A375 cells grown in the absence of methionine (▲) show growth arrest due to lack of an essential amino acid in the medium. This is partially rescued by incubation with 100 μM MTA in control cells (●). MTA fails to rescue growth in cells in which MRDI expression is stably inhibited by shRNA (◇), demonstrating a requirement for MRDI in methionine salvage. *B*, MRDI-shRNA knockdown cells were grown in the presence of MTA and the absence of methionine. Growth was rescued by add-back expression of MRDI-WT (♦) but not C168S (■) or D248A (○) mutants, indicating that MRDI catalytic activity is needed for cell growth via methionine salvage. *C–H*, A375 cells grown as spheroids show suppression of invasion into 3D collagen matrix upon stable knockdown of MRDI with shRNA. The invasion phenotype is rescued equally well by MRDI-WT, -C168S, and -D248A, indicating that catalytic activity is not required for cell invasion.

metastatic tumors, revealing a role for RhoA signaling that is distinct from the previous characterization of RhoC in promoting melanoma metastases. The results underscore the importance of monitoring Rho-GTP levels given that the pathway activation in metastatic cell lines was not reflected by Rho protein expression. Rho activity assays are not routinely measured in cancer samples because of difficulties in performing GTP binding assays on tissue specimens. Future studies are needed to examine whether MRDI is a useful marker for Rho activation in clinical samples.

A completely unexpected finding was that MRDI has promiscuous function, acting both as a metabolic enzyme and a regulator of signal transduction. Enzymatic pathways involved in catabolism of MTA are ancient, having been delineated in bacteria and Archaea where they convert MTRu-1-P to 2-keto-4-methylthiobutyrate as a precursor of methionine (40). In contrast, pathways for methionine salvage in humans are incompletely defined, and many of the enzymes that make up these pathways have not been mapped in mammalian genomes. Thus, metabolic conversion of MTR-1-P to MTRu-1-P has been demonstrated in rat cell extracts (31), but the isomerase responsible for this conversion has not been identified until now. By showing that MRDI catalyzes the conversion of MTR-1-P to MTRu-1-P and demonstrating the dependence of activity on residues Cys^{168} and Asp^{248}, we identified the human MTR-1-P isomerase as well as confirmed residues in the enzyme active site. By showing that MRDI is required for growth in MTA in methionine-free medium and that growth depends on the Cys and Asp residues, we confirmed that MRDI functions as a necessary component in the pathway for methionine salvage from decarboxylated *S*-AdoMet. Thus, MRDI joins a handful of metabolic enzymes with "moonlighting" function in signal transduction (46).

MTR-1-P isomerase is not the only methionine salvage enzyme to be implicated in cancer. MTA phosphorylase, which catalyzes the conversion of MTA + $P_i \rightarrow$ MTR-1-P + adenine, is deficient in many cancer types including melanoma, often accompanying co-deletion in the chromosome 9q21 region with p19INK4/CDKN2A (46, 47). MTA phosphorylase is a target for development of inhibitors, which induce apoptosis in head and neck cancer cells, and loss of enzyme enhances cellular sensitivity to chemotherapeutic compounds (47–49). The mechanisms for cell toxicity have been variously ascribed to suppression of MTA recycling to *S*-AdoMet via methionine or inhibition of purine salvage initiated by the adenine product of MTA phosphorylase. MTA phosphorylase also has tumor suppressor function in certain cancer cells ascribed to autocrine effects of MTA buildup on growth factor and matrix metalloproteinase induction (50, 51). Our results are in contrast to the example of MTA phosphorylase because we showed unequivocally that MRDI controls cancer cell behavior in a manner that is independent of its catalytic function. We speculate that MRDI elevates cell invasion via protein-protein interactions mediated by surface residues distal to the enzyme active site. Thus, MRDI provides unique evidence that some of the processes regulating control of cell adhesion and motility by signal transduction pathways have evolved from protein scaffolds with ancient metabolic function.

Acknowledgments—We are indebted to Lucy Ghoda, Indranil Basu, Vern Schramm, Channing Der, Joan Heller Brown, and Amy Abell for reagents and advice with assays and to Emily Anderson, Carrie Croy, and Anastasia Khvorova for help in facilitating RNAi experiments. We also thank Meenhard Herlyn for the gift of FM melanocyte and WM melanoma cell lines and David Rimm and the Yale tissue microarray facility for providing us with access to melanoma tissue microarrays. Finally we thank Richard Shoemaker for invaluable assistance with NMR.

* This work was supported, in whole or in part, by National Institutes of Health Grants R01-CA118972 (to N. G. A.), R01-AI060841 (to M. C. S.), R01-CA126240 (to K. A. R.), P50-CA058187 (to D. C.), T32-GM008759 (to P. D. T.), F32-CA112847 (to E. S. W.), and F32-CA105796 (to G. M. A.).

S The on-line version of this article (available at http://www.mcponline.org) contains supplemental material.

† Deceased January 8, 2009.

[b] Present address: Division of Applied Biochemistry, Dept. of Bioproductive Science, Utsunomiya University, Tochigi 321-8505, Japan.

[d] Present address: OSI Pharmaceuticals Inc., 1 Bioscience Park Dr., Farmingdale, NY 11735.

[f] Present address: Orion Pharma, Orionintiel, P.O. Box 65, FI-02101 Espoo, Finland.

[j] To whom correspondence should be addressed. Tel.: 303-492-4799; Fax: 303-402-2439; E-mail: natalie.ahn@colorado.edu.

REFERENCES

1. Bogenrieder, T., and Herlyn, M. (2002) Cell-surface proteolysis, growth factor activation and intercellular communication in the progression of melanoma. *Crit. Rev. Oncol. Hematol.* **44,** 1–15
2. Sauter, E. R., and Herlyn, M. (1998) Molecular biology of human melanoma development and progression. *Mol. Carcinog.* **23,** 132–143
3. Jaffe, A. B., and Hall, A. (2005) Rho GTPases: biochemistry and biology. *Annu. Rev. Cell Dev. Biol.* **21,** 247–269
4. Clark, E. A., Golub, T. R., Lander, E. S., and Hynes, R. O. (2000) Genomic analysis of metastasis reveals an essential role for RhoC. *Nature* **406,** 532–535
5. Ikoma, T., Takahashi, T., Nagano, S., Li, Y. M., Ohno, Y., Ando, K., Fujiwara, T., Fujiwara, H., and Kosai, K. (2004) A definitive role of RhoC in metastasis of orthotopic lung cancer in mice. *Clin. Cancer Res.* **10,** 1192–1200
6. Horiuchi, A., Imai, T., Wang, C., Ohira, S., Feng, Y., Nikaido, T., and Konishi, I. (2003) Up-regulation of small GTPases, RhoA and RhoC, is associated with tumor progression in ovarian carcinoma. *Lab. Invest.* **83,** 861–870
7. Malliri, A., and Collard, J. G. (2003) Role of Rho-family proteins in cell adhesion and cancer. *Curr. Opin. Cell Biol.* **15,** 583–589
8. Sahai, E., and Marshall, C. J. (2002) Rho-GTPases and cancer. *Nat. Rev. Cancer* **2,** 133–142
9. Kimura, K., Ito, M., Amano, M., Chihara, K., Fukata, Y., Nakafuku, M., Yamamori, B., Feng, J., Nakano, T., Okawa, K., Iwamatsu, A., and Kaibuchi, K. (1996) Regulation of myosin phosphatase by Rho and Rho-associated kinase (Rho-kinase). *Science* **273,** 245–248
10. Watanabe, N., Kato, T., Fujita, A., Ishizaki, T., and Narumiya, S. (1999) Cooperation between mDia1 and ROCK in Rho-induced actin reorganization. *Nat. Cell Biol.* **1,** 136–143
11. Palazzo, A. F., Cook, T. A., Alberts, A. S., and Gundersen, G. G. (2001) mDia mediates Rho-regulated formation and orientation of stable microtubules. *Nat. Cell Biol.* **3,** 723–729
12. Sanz-Moreno, V., Gadea, G., Ahn, J., Paterson, H., Marra, P., Pinner, S., Sahai, E., and Marshall, C. J. (2008) Rac activation and inactivation control plasticity of tumor cell movement. *Cell* **135,** 510–523
13. Sahai, E., and Marshall, C. J. (2003) Differing modes of tumour cell invasion have distinct requirements for Rho/ROCK signalling and extracellular proteolysis. *Nat. Cell Biol.* **5,** 711–719
14. Webb, D. J., Donais, K., Whitmore, L. A., Thomas, S. M., Turner, C. E., Parsons, J. T., and Horwitz, A. F. (2004) FAK-Src signalling through paxillin, ERK and MLCK regulates adhesion disassembly. *Nat. Cell Biol.* **6,** 154–161
15. Zamir, E., and Geiger, B. (2001) Molecular complexity and dynamics of cell-matrix adhesions. *J. Cell Sci.* **114,** 3583–3590
16. Playford, M. P., and Schaller, M. D. (2004) The interplay between Src and integrins in normal and tumor biology. *Oncogene* **23,** 7928–7946
17. Webb, D. J., Parsons, J. T., and Horwitz, A. F. (2002) Adhesion assembly, disassembly, and turnover in migrating cells. *Nat. Cell Biol.* **4,** E97–E100
18. Hsu, M. Y., Elder, D. E., and Herlyn, M. (1999) Melanoma: the Wistar melanoma (WM) cell lines. *Human Cell Culture* **1,** 259–274
19. Creasey, A. A., Smith, H. S., Hackett, A. J., Fukuyama, K., Epstein, W. L., and Madin, S. H. (1979) Biological properties of human melanoma cells in culture. *In Vitro* **15,** 342–350
20. Giard, D. J., Aaronson, S. A., Todaro, G. J., Arnstein, P., Kersey, J. H., Dosik, H., and Parks, W. P. (1973) In vitro cultivation of human tumors: establishment of cell lines derived from a series of solid tumors. *J. Natl. Cancer Inst.* **51,** 1417–1423
21. Herlyn, M., Balaban, G., Bennicelli, J., Guerry, D., 4th, Halaban, R., Herlyn, D., Elder, D. E., Maul, G. G., Steplewski, Z., and Nowell, P. C. (1985) Primary melanoma cells of the vertical growth phase: similarities to metastatic cells. *J. Natl. Cancer Inst.* **74,** 283–289
22. Satyamoorthy, K., DeJesus, E., Linnenbach, A. J., Kraj, B., Kornreich, D. L., Rendle, S., Elder, D. E., and Herlyn, M. (1997) Melanoma cell lines from different stages of progression and their biological and molecular analyses. *Melanoma Res.* **7,** Suppl. S2, S35–S42
23. Schaack, J., Langer, S., and Guo, X. (1995) Efficient selection of recombinant adenoviruses by vectors that express beta-galactosidase. *J. Virol.* **69,** 3920–3923
24. Singh, V., Shi, W., Evans, G. B., Tyler, P. C., Furneaux, R. H., Almo, S. C., and Schramm, V. L. (2004) Picomolar transition state analogue inhibitors of human 5′-methylthioadenosine phosphorylase and x-ray structure with MT-immucillin-A. *Biochemistry* **43,** 9–18
25. Elbashir, S. M., Harborth, J., Lendeckel, W., Yalcin, A., Weber, K., and Tuschl, T. (2001) Duplexes of 21-nucleotide RNAs mediate RNA interference in cultured mammalian cells. *Nature* **411,** 494–498
26. Qin, X. F., An, D. S., Chen, I. S., and Baltimore, D. (2003) Inhibiting HIV-1 infection in human T cells by lentiviral-mediated delivery of small interfering RNA against CCR5. *Proc. Natl. Acad. Sci. U.S.A.* **100,** 183–188
27. Kabuyama, Y., Polvinen, K. K., Resing, K. A., and Ahn, N. G. (2004) Two-dimensional gel electrophoresis for the identification of signaling targets. *Methods Mol. Biol.* **284,** 37–49
28. Blum, H., Beier, H., and Gross, H. J. (1987) Improved silver staining of plant proteins, RNA and DNA in polyacrylamide gels. *Electrophoresis* **8,** 93–99
29. Shevchenko, A., Wilm, M., Vorm, O., and Mann, M. (1996) Mass spectrometric sequencing of proteins silver-stained polyacrylamide gels. *Anal. Chem.* **68,** 850–858
30. Abramoff, M. D., Magelhaes, P. J., and Ram, S. J. (2004) Image processing with ImageJ. *Biophotonics Intl.* **11,** 36–42
31. Furfine, E. S., and Abeles, R. H. (1988) Intermediates in the conversion of 5′-S-methylthioadenosine to methionine in *Klebsiella pneumoniae*. *J. Biol. Chem.* **263,** 9598–9606
32. Ren, X. D., and Schwartz, M. A. (2000) Determination of GTP loading on Rho. *Methods Enzymol.* **325,** 264–272
33. Shah, V., Bharadwaj, S., Kaibuchi, K., and Prasad, G. L. (2001) Cytoskeletal organization in tropomyosin-mediated reversion of ras-transformation: Evidence for Rho kinase pathway. *Oncogene* **20,** 2112–2121
34. Kuhn, T. B., Meberg, P. J., Brown, M. D., Bernstein, B. W., Minamide, L. S., Jensen, J. R., Okada, K., Soda, E. A., and Bamburg, J. R. (2000) Regulating actin dynamics in neuronal growth cones by ADF/cofilin and rho family GTPases. *J. Neurobiol.* **44,** 126–144
35. Wittmann, T., Bokoch, G. M., and Waterman-Storer, C. M. (2004) Regulation of microtubule destabilizing activity of Op12/stathmin downstream of Rac1. *J. Biol. Chem.* **279,** 6196–6203
36. Kabuyama, Y., Langer, S. J., Polvinen, K., Homma, Y., Resing, K. A., and Ahn, N. G. (2006) Functional proteomics identifies protein tyrosine phosphatase 1B as a target of RhoA signaling. *Mol. Cell. Proteomics* **5,** 1359–1367
37. Ruth, M. C., Xu, Y., Maxwell, I. H., Ahn, N. G., Norris, D. A., and Shellman, Y. G. (2006) RhoC promotes human melanoma invasion in a PI3K/Akt-dependent pathway. *J. Invest. Dermatol.* **126,** 862–868
38. Miki, H., and Takenawa, T. (2003) Regulation of actin dynamics by WASP family proteins. *J. Biochem.* **134,** 309–313
39. Kyrpides, N. C., and Woese, C. R. (1998) Archaeal translation initiation revisited: the initiation factor 2 and eukaryotic initiation factor 2B alpha-beta-delta subunit families. *Proc. Natl. Acad. Sci. U.S.A.* **95,** 224–228
40. Sekowska, A., Dénervaud, V., Ashida, H., Michoud, K., Haas, D., Yokota, A., and Danchin, A. (2004) Bacterial variations on the methionine salvage pathway. *BMC Microbiol.* **4,** 9
41. Trackman, P. C., and Abeles, R. H. (1983) Methionine synthesis from 5′-S-Methylthioadenosine. Resolution of enzyme activities and identification of 1-phospho-5-S methylthioribulose. *J. Biol. Chem.* **258,** 6717–6720
42. Ashida, H., Saito, Y., Kojima, C., Kobayashi, K., Ogasawara, N., and

Yokota, A. (2003) A functional link between RuBisCO-like protein of Bacillus and photosynthetic RuBisCO. *Science* **302,** 286–290
43. Bumann, M., Djafarzadeh, S., Oberholzer, A. E., Bigler, P., Altmann, M., Trachsel, H., and Baumann, U. (2004) Crystal structure of yeast Ypr118w, a methylthioribose-1-phosphate isomerase related to regulatory eIF2B subunits. *J. Biol. Chem.* **279,** 37087–37094
44. Tamura, H., Saito, Y., Ashida, H., Inoue, T., Kai, Y., Yokota, A., and Matsumura, H. (2008) Crystal structure of 5-methylthioribose 1-phosphate isomerase product complex from *Bacillus subtilis*: implications for catalytic mechanism. *Protein Sci.* **17,** 126–135
45. Smalley, K. S., Haass, N. K., Brafford, P. A., Lioni, M., Flaherty, K. T., and Herlyn, M. (2006) Multiple signaling pathways must be targeted to overcome drug resistance in cell lines derived from melanoma metastases. *Mol. Cancer Ther.* **5,** 1136–1144
46. Moore, B. (2004) Bifunctional and moonlighting enzymes: lighting the way to regulatory control. *Trends Plant Sci.* **9,** 221–228
47. Della Ragione, F., Russo, G., Oliva, A., Mastropietro, S., Mancini, A., Borrelli, A., Casero, R. A., Iolascon, A., and Zappia, V. (1995) 5′-Deoxy-5′-methylthioadenosine phosphorylase and p16INK4 deficiency in multiple tumor cell lines. *Oncogene* **10,** 827–833
48. Chen, Z. H., Zhang, H., and Savarese, T. M. (1996) Gene deletion chemoselectivity: codeletion of the genes for p16(INK4), 1996. methylthioadenosine phosphorylase, and the alpha- and beta-interferons in human pancreatic cell carcinoma lines and its implications for chemotherapy. *Cancer Res.* **56,** 1083–1090
49. Chen, Z. H., Olopade, O. I., and Savarese, T. M. (1997) Expression of methylthioadenosine phosphorylase cDNA in p16−, MTAP− malignant cells: restoration of methylthioadenosine phosphorylase-dependent salvage pathways and alterations of sensitivity to inhibitors of purine de novo synthesis. *Mol. Pharmacol.* **52,** 903–911
50. Basu, I., Cordovano, G., Das, I., Belbin, T. J., Guha, C., and Schramm, V. L. (2007) A transition state analogue of 5′-methylthioadenosine phosphorylase induces apoptosis in head and neck cancers. *J. Biol. Chem.* **282,** 21477–21486
51. Stevens, A. P., Spangler, B., Wallner, S., Kreutz, M., Dettmer, K., Oefner, P. J., and Bosserhoff, A. K. (2009) Direct and tumor microenvironment mediated influences of 5′-deoxy-5′-(methylthio)adenosine on tumor progression of malignant melanoma. *J. Cell. Biochem.* **106,** 210–219